ELSEVIER

Biophysical Chemistry 122 (2006) 79–89

Biophysical Chemistry

http://www.elsevier.com/locate/biophyschem

Characterization of the kinetics of phospholipase C activity toward mixed micelles of sodium deoxycholate and dimyristoylphosphatidylcholine

Radha Ranganathan [a,*], Celize Maia Tcacenco [a], Renato Rosseto [b], Joseph Hajdu [b]

[a] Department of Physics and Astronomy and Center for Supramolecular Studies, California State University, Northridge, CA 91330-8268, USA
[b] Department of Chemistry and Center for Supramolecular Studies, California State University, Northridge, CA 91330-8262, USA

Received 3 February 2006; received in revised form 24 February 2006; accepted 24 February 2006
Available online 23 March 2006

Abstract

Phospholipase C catalyzed hydrolysis of dimyristoyl phosphatidylcholine (DMPC) in phospholipid–bile salt mixed micelles was studied with particular attention on the relationship between interfacial enzyme activity and the physicochemical properties of substrate aggregates. Steady state kinetics is observed and it is argued that conditions for steady state exist because the enzyme encounters a steady supply of substrate by hopping between micelles at a rate faster than the chemical reaction rate. An existing kinetic model is reformulated to a more usable form. This presents a new approach to treating the kinetic data and allows extraction of the kinetic parameters of the model from the activity dependence on micellar lipid substrate surface concentration. The kinetic parameters were found to depend on the physicochemical properties of substrate aggregates, but remain constant over a range of lipid and bile salt concentrations. The substrate aggregates were characterized by time-resolved fluorescence quenching (TRFQ). The activity values and the micelle sizes group into two sets: (i) larger micelles for bile salt/lipid ≤ 5 showing higher activity and shorter steady state duration (≤ 4 min) and (ii) smaller micelles for bile salt/lipid > 5 with lower activity and longer steady state (≈ 10 min). At least two sets of parameters, for bile salt/lipid ≤ 5 and >5, characterize the kinetics. Higher enzyme–micelle dissociation constant and lower catalytic rate are found for the group of smaller micelles. An explanation supporting our finding is that as micelles become smaller the overlap area for enzyme–micelle binding decreases, leading to weaker binding. Consequently the enzyme dissociation constant increases. Extension of the present approach to other phospholipases and substrates to establish its generality and correlation between micelle size and the catalytic rate are areas for future investigations.

Keywords: Phospholipase; Phospholipid; Enzyme kinetics; Hydrolysis; Bile salts; Mixed micelles

1. Introduction

Phospholipases are a superfamily of lipolytic enzymes that catalyze phospholipid hydrolysis [1]. The uniqueness of these enzymes is that their activity is thousand fold or more enhanced when the lipid substrate is in an aggregated form as vesicles or in mixed micelles with other surfactants [2–5]. Enzymatic action occurs at the aggregate/water interface. For this reason the phospholipases are classified as interface enzymes [1]. In this work a kinetic investigation of the activity of the bacterial phospholipase C enzyme at the lipid water interface of lipid/bile salt aggregates in water and its correlation with the physicochemical properties of the substrate aggregate are conducted. Experiments include both enzyme activity and substrate characterization measurements. Time-resolved fluorescence quenching methods are employed to characterize the substrate aggregate and results are used in interpreting the kinetic data. A problem in seeking a correlation between microstructure and kinetics is that the microstructure changes during the course of enzyme activity and therefore it may not be a good parameter. However, we do observe an initial linear product formation vs. time curve and it is this initial activity that we address in this work. The duration of linearity (steady state) increases as the bile salt to lipid ratio increases. The velocities (slope of product vs. time) derived from the linear regions at various bile salt/lipid ratios are examined against a kinetic model and the kinetic parameters are extracted. Our goal is to understand not only the

* Corresponding author. Department of Physics, MD 8268, California State University, Northridge, CA 91330, USA. Tel.: +1 818 677 2942; fax: +1 818 677 3234.
E-mail address: radha.ranganathan@csun.edu (R. Ranganathan).

0301-4622/$ - see front matter © 2006 Elsevier B.V. All rights reserved.
doi:10.1016/j.bpc.2006.02.012

substrate concentration effect but also the differences in the characteristics of the kinetics between different bulk bile salt to lipid concentration ratios that are due to effects other than the substrate concentration effect. A question that is addressed in this work is the existence of conditions for steady state for micellar substrates, concerns about which were raised by Jain et al. [6]. A basic requirement for the existence of steady state kinetics is that substrate replenishment must occur at a faster rate than the chemical conversion rate [6]. In micellar aggregates, the number of lipid molecules in an aggregate is typically less than fifty. So either the enzyme must hop between micelles or the lipids must exchange between micelles at a suitable rate to satisfy this requirement. The observation of steady state means that the enzyme "sees" all the micelles. Furthermore, the effects of polydispersity in micelle size and composition are averaged out and one may derive a set of kinetic parameters from the initial linear regions of kinetics at various bile salt to lipid ratios.

The model used to analyze the kinetic data treats the interface as a cofactor and was originally applied towards the study of kinetics of phospholipase A_2 activity on Triton X-100/phospholipid micelles [3] and later, on sodium cholate/lipid micelles [4]. We begin with a recasting of the equation for the initial rate of hydrolysis to reveal a straightforward dependence on the surface concentration of lipids in a form that is more accessible for analysis of experimental data. With this new form it is shown that the kinetic parameters of the model can be individually determined, which was not possible before without making assumptions concerning the headgroup surface areas [3]. In earlier work the kinetic parameters were determined in a combined form [4]. The significance of determining the kinetic parameter, namely the catalytic rate, denoted by k_3 in this work, is that the effect of the biophysical property of the aggregate on k_3 can be investigated and this can lead to mechanistic models for enzyme activation. The kinetic parameters show a correlation with micelle size. The idea developed is that larger micelle size promotes stronger enzyme–micelle binding because of increased availability of overlap area. This restricts the enzyme from intermicellar hopping and leading to non-steady state conditions. However continued presence of activity is observed over long periods of time at all concentrations studied in this work. Thus a clearer picture of the nature of involvement of the micellar interface emerges.

The enzyme selected in this investigation is bacterial phospholipase C (PLC) isolated from *Bacillus cereus*. The reason for beginning our studies with PLC is that this enzyme does not require calcium as a cofactor unlike the more widely investigated lipolytic enzyme, phospholipase A_2. Added salts are known to change micelle microstructure [7]. In beginning our investigations on the role of micelle microstructure, this additional complication due to calcium is avoided by the choice of PLC. Lipid/bile salt aggregates are the natural substrates for the digestive enzymes and are chosen as the substrate for our investigations [1]. The lipid substrate, dimyristoylphosphatidylcholine (DMPC), is solubilized in micelles of the bile salt, sodium deoxycholate (NaDC). The chemical reaction involves the hydrolysis of the phosphodiester bond as described in Eq. (1) below. The products released are dimyristoyl glycerol and phosphorylcholine. The latter is the acidic function that is titrated with sodium hydroxide to measure the activity of the enzyme.

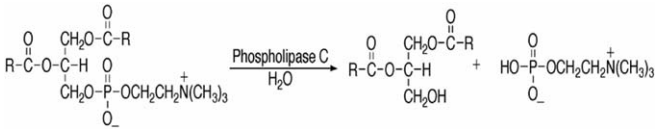

(1)

1.1. The kinetic model

The model of interface enzyme kinetics, based on the putative Michaelis–Menten scheme, first proposed by Deems et al. is presented below. Three steps define the process [3]:

(i) Enzyme binds to the micelle interface to form a micelle bound enzyme, E^*_{mic}

$$[E] + n[\text{micelles}] \underset{k_{-1}}{\overset{k_1}{\rightleftarrows}} [E^*_{mic}], \tag{2}$$

n is the number of binding sites per micelle, [micelles] is the concentration of micelles.

(ii) The bound enzyme binds a substrate lipid in the aggregate, forming the complex $E^*_{mic}S$. [S] is the interface substrate concentration.

$$[E^*_{mic}] + [S] \underset{k_{-2}}{\overset{k_2}{\rightleftarrows}} [E^*_{mic}S]. \tag{3}$$

(iii) The enzyme catalyzes hydrolysis of the lipid in the chemical step, forming the product P.

$$[E^*_{mic}S] \xrightarrow{k_3} [E^*_{mic}] + [P] \tag{4}$$

The E^*_{mic} on the right side of Eq. (3) is still bound to the micelle and can dissociate through the reverse reaction step of Eq. (2). The enzyme activity is defined by the rate of product formation, v, per mole of enzyme present, that is $v/[E_T]$, where $[E_T]$ is the total enzyme concentration. The steady state solution for the activity at the aggregate interface is

$$\text{Activity} = \frac{v}{[E_T]} = \frac{k_3 n[\text{micelles}][S]}{K_S K_M + K_M n[\text{micelles}] + n[\text{micelles}][S]} \tag{5}$$

and its inverse is

$$\frac{[E_T]}{v} = \frac{K_S K_M}{k_3 n[\text{micelles}][S]} + \frac{K_M}{k_3[S]} + \frac{1}{k_3} \tag{6}$$

$$K_S = k_{-1}/k_1; K_M = \frac{k_{-2} + k_3}{k_2}. \tag{7}$$

The steady state solution, Eq. (5), clearly shows that the activity depends explicitly on the three physicochemical properties of micelles: the number of binding sites, n; the concentration of micelles, [micelles]; and the interface lipid concentration in the micelle, [S]. Previous studies have used the

equations in the form displayed in Eqs. (5) and (6), which require designing a series of samples with a variation in one variable while the other two are constant [3,4]. This is not always practical. We now proceed to show that a simplification ensues when we consider that the three variables are interrelated because the lipid surface concentration is the number of moles of lipid molecules per micelle per unit surface area of micelle and n depends on the micelle surface area. Thus [S] depends, not only on the bulk lipid concentration, but also on the concentration of micelles and the micelle surface area. This is expressed by,

$$[S] = \frac{[\text{lipid}]}{[\text{micelles}]A_{\text{micelle}}N_0}, \tag{8}$$

where, [lipid] is the bulk lipid concentration, A_{micelle} is the micelle surface area and N_0 is Avogadro's number. The number of binding sites per micelle, n, is the ratio of micelle surface area to the area per binding site. Thus,

$$n = \frac{A_{\text{micelle}}}{a_0}. \tag{9}$$

The area per binding site, a_0, may be treated as the projection of the enzyme's cross-sectional area on to the micelle surface [3]. The identifications of [S] and n as in Eqs. (8) and (9) give for the product n[micelles][S],

$$n[\text{micelles}][S] = \frac{A_{\text{micelle}}}{a_0}[\text{micelles}]\frac{[\text{lipid}]}{[\text{micelles}]A_{\text{micelle}}N_0} = \frac{[\text{lipid}]}{a_0N_0}. \tag{10}$$

The result in Eq. (10) allows a rewriting of Eqs. (5) and (6) in the forms,

$$\frac{v}{[E_T]} = \frac{k_3[S]}{C_1k_3[S] + K_M}. \tag{11}$$

where,

$$C_1 = \frac{K_SK_Ma_0N_0}{k_3[\text{lipid}]} + \frac{1}{k_3}. \tag{12}$$

Apart from the constants a_0 and N_0, C_1 contains only the kinetic parameters and the total lipid concentration. The reciprocal of the activity is,

$$\frac{[E_T]}{v} = \frac{K_SK_Ma_0N_0}{k_3[\text{lipid}]} + \frac{K_M}{k_3[S]} + \frac{1}{k_3} = C_1 + \frac{K_M}{k_3}\left(\frac{1}{[S]}\right), \tag{13}$$

For a series of concentrations where [lipid] is constant and the [bile salt] is varied, the activity itself should show a saturation behavior according to Eq. (11). A plot of the reciprocal of the activity vs. the reciprocal of the lipid surface concentration should be linear with slope$=K_M/k_3$ and intercept$=C_1$. A plot of C_1 vs. 1/[lipid] has a slope $= \frac{K_SK_Ma_0N_0}{k_3}$ and intercept$=1/k_3$.

Combining the slope K_M/k_3 of the double reciprocal plot together with slope and intercept of C_1 vs. 1/[lipid] yields the individual values of K_S, K_M, and k_3.

A further reduction occurs upon a consideration of the different terms in Eq. (8) for [S]. The micelle concentration is,

$$[\text{micelles}] = \frac{[\text{bile salt}]-\text{IMC}}{N_{\text{bs}}}, \tag{14}$$

where [bile salt] is the total bulk concentration of bile salt, IMC is the intermicellar concentration of bile salt, and N_{bs} is the aggregation number of bile salt molecules in a micelle. The area of the micelle is,

$$A_{\text{micelle}} = N_{\text{bs}}a_{\text{bs}} + N_{\text{lipid}}a_{\text{lipid}}, \tag{15}$$

where N_{lipid} is the number lipid molecules solubilized in an aggregate and a_{bs} and a_{lipid} are the surface areas of the bile salt and lipid headgroup, respectively. Furthermore, N_{lipid} is given by

$$N_{\text{lipid}} = \frac{[\text{lipid}]}{[\text{micelles}]} = \frac{[\text{lipid}]N_{\text{bs}}}{[\text{bile salt}]-\text{IMC}}, \tag{16}$$

where Eq. (14) is used to obtain the second equality.

Introducing Eqs. (14)–(16), in to Eq. (8), gives

$$[S] = \frac{[\text{lipid}]}{a_{\text{bs}}([\text{bile salt}]-\text{IMC}) + [\text{lipid}]a_{\text{lipid}}}, \qquad \frac{1}{[S]} = a_{\text{bs}}\frac{[\text{bile salt}]-\text{IMC}}{[\text{lipid}]} + a_{\text{lipid}}. \tag{17}$$

Apart from the bulk concentrations and molecular surface areas the only physicochemical property needed to determine [S] is the intermicellar concentration of bile salt. This renders the calculation of [S] and thus Eqs. (5) and (6) through the forms Eqs. (11) and (13) easily usable. According to Eq. (13), for a series of samples with constant [lipid] and varying [bile salt], the slope, K_M/k_3, of the reciprocal of the activity vs. 1/[S], is not affected by the value of IMC, but the intercept ($=C_1$) is.

The equations in the form of Eqs. (13) and (17) offer a method to determine the kinetic parameters K_M, k_3, and K_S. The slopes of the reciprocal of the activity vs. 1/[S] for different series of samples each with a constant [lipid] and varying [bile salt] gives the slope K_M/k_3. Such a series is easily prepared. Then the intercepts, C_1 (Eq. (12)), of each of the plots vs. 1/[lipid], yields the individual values of K_S, K_M and k_3.

2. Materials and methods

2.1. Chemicals

The bile salt utilized was sodium deoxycholate, NADC, (Sigma), the phospholipid was dimyristoylphosphatidylcholine, DMPC (Avanti), and the enzyme was bacterial Phospholipase C, PLC (*B. cereus* — Sigma-Aldrich). The fluorescent probe used for the physicochemical characterization of the substrates by time-resolved fluorescence quenching was pyrene and the quencher was a nitroxide labeled phospholipid whose structure is shown in Fig. 1 [8].

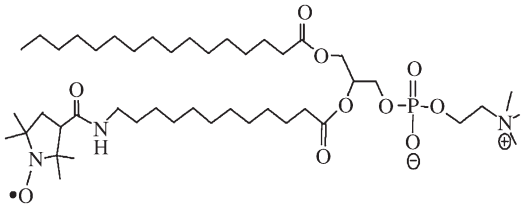

Fig. 1. The quencher lipid. The nitroxide free radical attached to the fatty acid tail quenches the fluorescence emission from pyrene [8].

2.2. Mixed micelle solution preparation

In a Potter–Elvehjeim tube, a dried film of DMPC is mixed with the NaDC solution and homogenized by stroking twenty times with the Teflon pestle of the homogenizer. The compositions and concentrations investigated were (i) [DMPC]=2 mM and NaDC ranging from 10 to 50 mM, (ii) [DMPC]=4 mM and NaDC ranging from 10 to 50 mM, and (iii) [DMPC]=6 mM and NaDC ranging from 10 to 40 mM.

2.3. Enzyme kinetics

Studies of the kinetics of enzymatic hydrolysis of DMPC in DMPC/NaDC mixed micelles by bacterial PLC were conducted employing the pH–stat method [4]. The enzyme was dialyzed for three days in a 0.05 M phosphate buffer at pH 8, changing the buffer every 8 h. The solution of the PLC was stored at 4 °C and the protein concentration was determined by the method of Lowry et al. using the bovine serum albumin (BSA) as a standard [9]. The activity of the enzyme stock solution was routinely checked with a standard egg yolk emulsion assay [10]. The activity is the amount of phosphorylcholine released per milligram of enzyme per unit time. It is measured in units of μmol of acid released, due to lipid hydrolysis, per minute per milligram of enzyme (μmol/min/mg). Expressed in these units it is equivalent to $v/[E_T]$ of Eqs. (5) and (11). The activity of the enzyme in the standard egg yolk assay was 600 μmol/min/mg.

The activity of PLC in mixed micelles of NaDC/DMPC was measured by addition of 250 μL of enzyme (0. 67 μg) into 5 mL of mixed micelles solutions, and monitoring the amount of 0.01 M NaOH required per minute to maintain a constant pH of 8 using a Radiometer pH–stat assembly consisting of a titrator, an auto burette, and pH meter, Model 290 PHM, interfaced to a computer for recording data [4]. The basis for this method is that the phosphorylcholine released by the action of the enzyme causes the pH to drop and the amount of NaOH needed to bring the pH back to a preset value is a measure of enzyme activity. The reaction was followed for 10 min. The initial rate of activity was determined from the first 2 to 4 min of data. The yield increases linearly with time and the slope of the line divided by the mass of the enzyme in mg gives the activity, in units of μmol/min/mg. The assay was conducted at 40 °C.

2.4. Time-resolved fluorescence quenching (TRFQ)

It may appear from Eqs. (11) and (17) that microstructural characterization of micelles is not necessary, because the only micellar property that appears explicitly is the IMC. It turns out however that the kinetic parameters K_S, K_M, and k_3 are affected by micelle microstructure. TRFQ characterization also helps in the determination of the criteria for the existence of steady state conditions. This is shown to involve K_S, micelle size and concentration.

In the course of the past few decades TRFQ has been established as a direct technique to determine micelle aggregation numbers and bimolecular reaction rates in micelles [11–14]. In the TRFQ method fluorescence probes and quenchers, being themselves hydrophobic, are dispersed in micelles and the quenched time-decay of the probe fluorescence is measured. Under the conditions that (i) micelle size is monodisperse, (ii) probes and quenchers occupy the micelles according to Poisson statistics and (iii) the probes and quenchers do not migrate between micelles within the lifetime of the probe fluorescence, the quenched decay of the fluorescence, $F(t)$, is given by the Infelta model [11,15–19].

$$F(t) = F(0)\exp[-k_0 t - A_3\{1-\exp(-k_q t)\}]. \quad (18)$$

The decay rate k_0 is the rate of pyrene fluorescence decay in micelles with zero quencher occupation, k_q is the decay rate due to quenching by one quencher, and is thus the quenching rate constant. The Infelta quenching model (Eq. (18)) is basically an analytical sum of exponential decays of fluorescence in micelles with zero quenchers (decay rate, k_0), one quencher (decay rate, k_q), two quenchers (decay rate 2 k_q), and so on, where the number of micelles with a number n of quenchers is given by a Poisson distribution. The quantity A_3 is the average number of quenchers per micelle. A fit of Eq. (18) to the quenched decay curve returns k_0, k_q, and A_3. The physicochemical properties of micelles that are relevant to the goals of this work are:

1. Concentration of micelles, [micelles]. The quencher concentration, $[Q]$, is a known sample parameter. Using the fitted value of A_3, and the known $[Q]$, the concentration of micelles may be calculated from

$$[\text{micelles}] = [Q]/A_3. \quad (19)$$

2. Bimolecular collision rate in a micelle and the micelle size. (i) fluorescence quenching is diffusion controlled and as such the quenching rate constant, k_q, determined from the fits to the quenched decay curve is given by the bimolecular collision rate between probe and quencher, (ii) the larger the size of the micelle, the smaller is the probe–quencher encounter rate; thus k_q is inversely proportional to micelle size and has been observed to be so in all TRFQ experiments [20–25]. This is proven besides being intuitive. Therefore k_q^{-1} is a measure of micelle size, that is,

$$\text{micelle size} \propto k_q^{-1} \quad (20)$$

A numerical value of size is not used anywhere in this work. k_q^{-1} is used as an indicator of micelle size and to aid interpretation of the activity data.

3. The inter-micellar concentration of bile salt. The micelle concentration determined from the fits to the experimental decay data according to Eq. (19) is related to the bulk bile salt concentration through Eq. (14). A plot of [micelles] vs. [bile salt] may be used to determine N_{bs} and the IMC, if the plot is found to be linear. In a first approximation, over a small range of bile salt concentration, if N_{bs} is assumed to be constant then N_{bs} and IMC may be computed from the slope and intercept of [micelles] vs. [bile salt]. The details of the procedure used to determine the listed micelle properties are given in an Appendix.

The fluorescence decay curves of pyrene were obtained using a nanosecond flashlamp FL900 lifetime measurement spectrometer of Edinburgh Analytical Instruments. Pyrene fluorescence was excited by nanosecond pulses from a flashlamp enclosed in hydrogen atmosphere. The excitation monochromator was centered at 335 nm. The fluorescence emission was measured by time-correlated single photon counting with the emission monochromator centered at 372 nm. The decay curves were corrected for instrument response and then analyzed using Eq. (18) and polydispersity was treated according to the details in the Appendix which includes sample fluorescence decay data and fitted curves. The mixed micellar substrate aggregates of DMPC and NaDC were characterized at 40 °C. All samples were degassed to remove dissolved oxygen in order to eliminate the quenching of pyrene fluorescence by oxygen. The de-oxygenation was accomplished by a sequence of freezing the sample, pumping on the sample, followed by thawing. The freeze, pump, thaw sequence was repeated three times.

3. Results and discussion

3.1. Reaction progress curves

The time dependence of the amount of product released due to enzymatic hydrolysis of DMPC, dispersed in sodium deoxycholate (NaDC) bile salt micelles, by *B. cereus* phospholipase C, measured as described in Section 2.3, is shown in Fig. 2 for the three series of samples. In each of the series, [lipid] was held constant and [NaDC] was varied from 10 to 50 mM. A marked change in behavior is observed at about [NaDC] = 25 mM. For [NaDC] ≥ 25 mM, the reaction progress curve is linear over 8 to 10 min, signifying a long lived steady state. A clear demarcation at [NaDC] ≈ 25 mM is seen which is particularly obvious in the case of [DMPC] = 2 mM. The reaction rate given by the slope of the graphs in Fig. 2, decreases as [NaDC] is increased. There is no latency period in activity as observed in the case of bilayer and large vesicular substrates. The latency period followed by a burst of activity has been attributed to the build up of reaction products that induce surface irregularities which aid in enzyme binding [26–28].

3.2. Activity

The initial rate of hydrolysis was determined as the slope of the reaction vs. time curves in the first 4 min for the higher

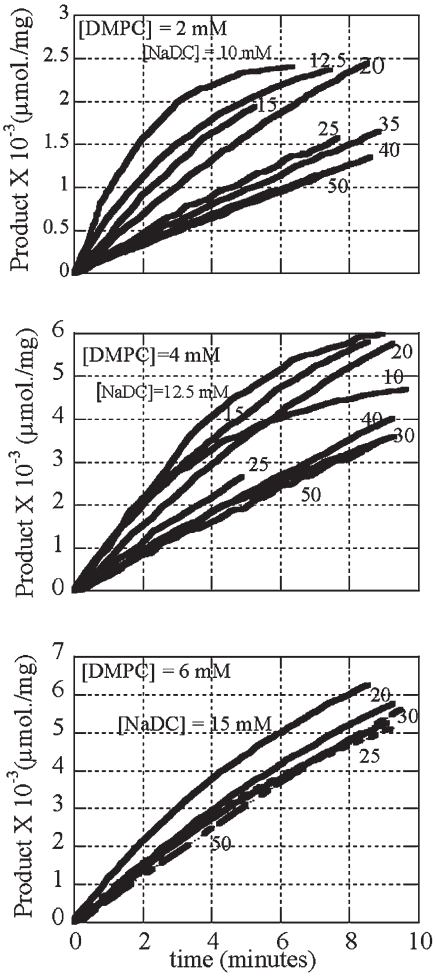

Fig. 2. Reaction progress curves in three series of samples, each with a constant [DMPC] and varying [NaDC] as shown. The *Y*-axis represents the amount, in µmol, of phosphorylcholine released per mg of enzyme, following catalytic hydrolysis of DMPC by bacterial phospholipase C at 40 °C.

[NaDC] samples which show a long lived steady state. For the lower [NaDC] cases, the first 1 to 2 min were used. The activity was then calculated as the slope divided by the mass of enzyme in solution (Section 2.3) and represents $v/[E_T]$ of Eqs. (5) and (11). Fig. 3 shows the activity as a function of [NaDC] for each of the constant [DMPC] series. The activity decreases more steeply between [NaDC] = 10 and 25 mM than for [NaDC] > 25 mM.

3.3. Micelle size and correlation with activity

TRFQ allows the determination of the micelle aggregation number, which in this case is the sum of the number of bile salt and lipid molecules per micelle, $N_{bs}+N_{lipid}$, from the experimentally determined [micelles], the IMC, and the operational definitions in Eqs. (14) and (16). The inverse of the quenching rate constant, k_q, as described in Section 2.4, is a measure of the geometrical size of the micelle (Eq. (20)). It is generally known that lipid/bile salt mixed micelle size decreases as the bile salt to lipid ratio increases [29]. This is because the micelle concentration increases as more detergent is added and thereby

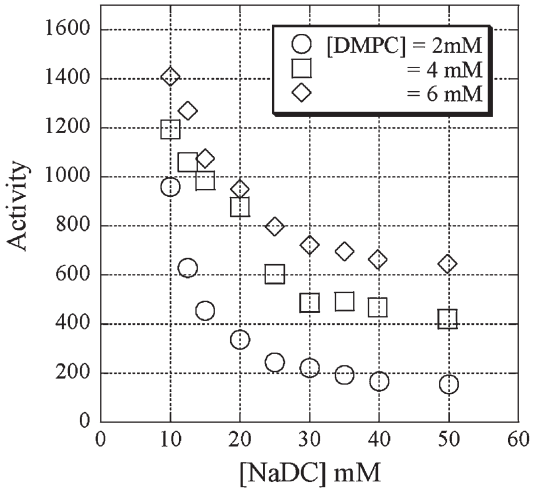

Fig. 3. The activity (in units of μmol of phosphorylcholine released per minute per mg of enzyme) of *Bacillus cereus* phospholipase C vs. the concentration of the bile salt, NaDC, at constant [DMPC].

the number of lipid molecules per micelle decreases. Neither the aggregation number nor the physical micelle size is actually needed for applying the final equation for the velocity (Eqs. (11)–(13)) to the kinetic data. However the size information, even if it is only indirectly known through k_q^{-1} is useful in understanding the change in the kinetic behavior that occurs at [NaDC]=25 mM. The aggregation numbers for [NaDC] <25 mM were calculated and are discussed in the next section. TRFQ data showed clearly that micelle size decreases (k_q increases) more rapidly with increase in [NaDC] up to about [NaDC]=25 mM than in the region [NaDC]>25 mM. The size variation is shown in Fig. 4. The steepest drop in size occurs in the region 20 mM<[NaDC]<30 mM. We treat the micelles and [NaDC] concentration as belonging to either of two groups: larger micelles for [NaDC]<25 mM and smaller micelles [NaDC]>25 mM. This grouping is prompted by the observed

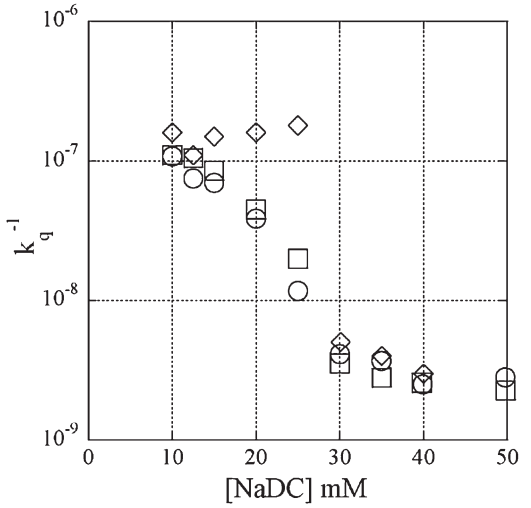

Fig. 4. Variation of micelle size as indicated by the fluorescence quenching rate, k_q^{-1}, with increase in [NaDC] and a constant [DMPC] of 2 mM (○); 4 mM (□); and 6 mM (◇). The fluorescence quenching rate was measured by time-resolved fluorescence quenching. The micelle size is proportional to k_q^{-1}.

distinctive behavior of activity between the same two concentration regions of [NaDC]<25 mM and [NaDC] >25 mM.

Examining the reaction progress curves and the activity data against such a grouping of micelle size shows that: (i) long lived steady state observed for [NaDC]>25 mM corresponds to the smaller micelles and (ii) the dependence of the activity on NaDC concentration shows a slower variation for the smaller micelles ([NaDC]>25 mM) than for the larger micelles present at [NaDC]<25 mM. This suggests that at least two sets of kinetic parameters, depending on detergent concentration, define the kinetics. Note that this correlation does not involve particular micelle sizes or microstructure but rather the reference is to whether the micelles are large or small.

3.4. Intermicellar concentration of NaDC and aggregation numbers

Table 1 gives the values of IMC and the bile salt aggregation numbers determined for NaDC/DMPC mixed micelles from the slope and intercept of the experimentally determined [micelles] vs. the total bile salt concentration [NaDC] according to Section 2.4 (item 3) for [NaDC]<25 mM. The details are given in the Appendix which includes the plots of [micelles] vs. [NaDC]. With the values of IMC and the bile salt aggregation number, N_{bs}, the lipid aggregation number N_{lipid}, for any particular bile salt/lipid mixture may simply be calculated using Eq. (16). The results (Appendix, Fig. 8) show that at any given lipid concentration (2, 4, or 6 mM) the concentration of micelles increases with [NaDC] and N_{bs} remains about constant. Because the samples are a constant [lipid] series, this means that N_{lipid} per micelle decreases as [micelles] increase with [NaDC]. Therefore this result together with Fig. 4 is evidence that the micelle size decreases as the lipid to bile salt ratio decreases.

3.5. Application of the kinetic model, Eqs. (11) and (13)

The substrate concentration was calculated using Eq. (17) with the values of IMC from Table 1, the bulk NaDC concentration, and with the surface areas for NaDC, a_{bs}=346 Å^2 and a_{lipid}=85 Å^2 [3,30]. The graphs in panels A and B of Fig. 5 show the plots of activity vs. [*S*] and 1/activity vs.1/[*S*], respectively, for [NaDC]≤25 mM. A saturation behavior is indicated in Fig. 5, panel A and a linear relation between the reciprocals in Fig. 5, panel B as predicted by Eqs. (11) and (13). Linear regression fits yield the slopes, K_M/k_3 and

Table 1
Intermicellar concentration (IMC) of NaDC in mixtures of NaDC and DMPC at three fixed DMPC concentrations at 40 °C

[DMPC]	IMC [a] (M)	N_{bs}
0.002	0.0087±0.0015	22
0.004	0.0082±0.0012	37
0.006	0.004±0.001	47

[a] The determination of IMC is based on Eq. (14) and is computed from the slope and intercept of a plot of [micelles] vs. [NaDC]. [micelles] is determined by TRFQ.

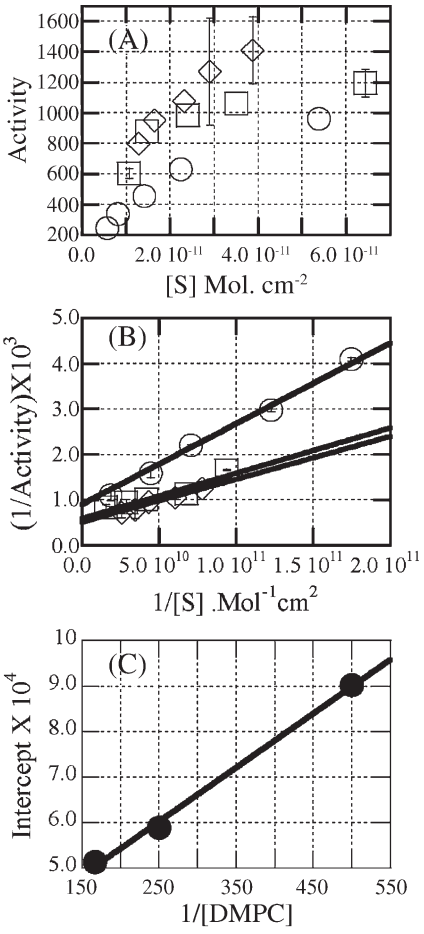

Fig. 5. Application of the kinetic model in the form, Eqs. (11) and (13) to the three series of samples with constant [DMPC] of 2 mM (○); 4 mM (□); and 6 mM (◇) and varying [NaDC] for 10 mM ≤ [NaDC] ≤ 0.25 mM. A. Activity vs. the lipid surface concentration, [*S*]. B. The double reciprocal plot of 1/activity vs. 1/[*S*]. (C) The intercept (C_1, Eq. (12)) of the plots in panel B vs. 1/[DMPC].

intercepts, C_1 for each of the lipid concentrations. The intercept, C_1 (Eq. (12)) is an algebraic package that is inversely proportional to [lipid], where the lipid in the present experiments is DMPC. Linear fits to the plot of the intercept, C_1 vs. 1/[DMPC] yields the slope $K_S a_0 N_0 \frac{K_M}{k_3}$ and intercept $1/k_3$. Using the values of K_M/k_3 determined as the slope of the double reciprocal plots obtained previously (Fig. 5, panel B), and the constants N_0 allows determination of K_S a_0, K_M, and k_3 individually. The values are listed in Table 2. The value of the area per binding site, a_0, is required to determine K_S from K_S a_0.

Table 2
Kinetic parameters of enzymatic hydrolysis of DMPC solubilized in NaDC micellar aggregates by bacterial phospholipase C at 40 °C

Concentration of NaDC	K_S a_0 (M cm^2)	K_S (M)[a]	K_M (mol. cm^{-2})	k_3 (μmol per min per mg)
10 mM ≤ [NaDC] ≤ 5 mM	8.5×10^{-17}	2×10^{-3}	4×10^{-11}	2249
25 mM < [NaDC] ≤ 50 mM	5.1×10^{-16}	1.2×10^{-2}	8×10^{-12}	849

[a] The values for K_S are calculated from $K_S a_0$ for $a_0 = 5\times85$ Å^2 (Section 3.5).

It is not available at present. If the overlap area is taken to be the area of about five phospholipid headgroups, $a_0 = 5\times85$ Å^2 [3], then the K_S is as reported in Table 2. Error in the value of a_0 gives rise to a systematic error in K_S.

A similar analysis was conducted on the data for [NaDC] >25 mM where small micelles are present. The variation of the activity with [*S*], Fig. 6 panel A, is slower than for [NaDC] ≤ 25 mM (Fig. 5 panel A). This results in a shallower slope in the 1/activity vs.1/[*S*] graph, Fig. 6 panel B. Calculations of the kinetic parameters for the smaller micelles yield a value of K_M that is an order of magnitude smaller and K_S an order of magnitude larger than those obtained for the larger micelles. The values are listed in Table 2.

The accuracy in the values of the kinetic parameters derived from the use of Eqs. (11)–(17) is limited by the accuracy in IMC and in the molecular surface areas. These are systematic errors. The error in IMC gives a systematic error to less than one order of magnitude.

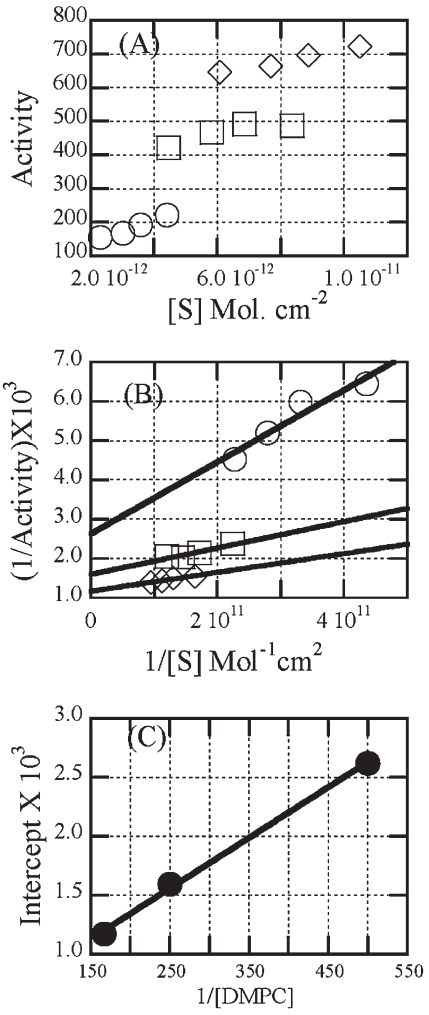

Fig. 6. Application of the kinetic model in the form, Eqs. (11) and (13) to the three series of samples with constant [DMPC] of 2 mM (○); 4 mM (□); and 6 mM (◇) and varying [NaDC] for 30 mM ≤ [NaDC] ≤ 0.50 mM. A. Activity vs. the lipid surface concentration, [*S*]. B. The double reciprocal plot of 1/activity vs. 1/[*S*]. C. The intercept (C_1, Eq. (12)) of the plots in panel B vs. 1/[DMPC].

The present results show that Eqs. (11) and (13) describe bacterial phospholipase C interface kinetics. The kinetic parameters are not constant over all concentrations because they are affected by the microstructure of the substrate aggregate which changes according to concentration. However the data could be grouped into two concentration regions of bile salt in both of the two independent experiments of enzyme activity and TRFQ. This classification yields two sets of kinetic parameters and steady state duration and two groups of micelle sizes. A correlation is therefore sought between the effect of micelle size and enzyme activity, beyond just the substrate surface concentration effect. Detergent mixed micellar substrates typically have a few lipid molecules per aggregate. In order to achieve steady state, the substrate should be replenished at a rate faster than the rate at which they are consumed [6]. If the enzyme is bound strongly to a micelle (low K_S) there is a waiting period after the first round of reaction with those lipids already present before the next supply of lipids which occurs either by exchange between micelles during inter micellar collisions or by the transfer between micelles through water. Both of these are slow processes compared to the catalytic conversion rate [31,32]. Therefore unless the enzyme is weakly bound and the inter micellar hopping of the micelle is at a rate faster than the catalytic rate, conditions for steady state are not present and the reaction would be completed in a very short time. The measurements presented in this work show the presence of continued activity over long periods of time. Therefore these results must mean that the enzyme dissociates from the micelle rapidly, corresponding to weak binding or high K_S. Furthermore, application of the kinetic model gives higher K_S values for the smaller micelles. K_S increases by an order of magnitude for the smaller micelles, indicating that enzyme/micelle binding depends on micelle size and gets weaker as the micelle becomes smaller. This may be understood when considering that as the micelle surface area decreases; the available enzyme/micelle overlap area will decrease causing the binding to become weaker with a concomitant faster intermicellar hopping rate. Another notable observation is the linearity in the reaction progress curves over longer times at the higher bile salt concentrations, where the micelles in general are smaller, than for larger micelles. A rapid replenishment rate and invariable kinetic parameters are conditions for continued activity and steady state kinetics. Microstructural changes due to the products formed can induce non-linearity through their effect on the kinetic parameters. This effect is more notable at the lower bile salt to lipid ratios because of the greater number of lipid molecules per aggregate and hence higher activity and thus an increased concentration of products. This investigation does not address the microstructural aspects like the ordering of lipids and the actual lipid conformation in the micelle. Rather the kinetic properties are determined for the microstructure, whatever it may be, according to the methods proposed and it is found that these properties do depend on the lipid to bile salt ratio. However within a limited concentration range they do remain constant as determined from the model. The differences in the values of the parameters between different concentration ranges may be attributed to the actual microstructure and is an area for future investigation.

4. Summary and conclusions

The model for interface enzyme activity first applied to investigate phospholipase A_2 [3] was adapted to study bacterial phospholipase C kinetics at bile salt/lipid interfaces. The principal outcomes of this work are: (i) Reduction of the equation for the activity dependence on substrate aggregate properties to show a more straightforward form in which the only micellar property explicitly present is the intermicellar concentration of the detergent. This is based on the model that the interface substrate concentration is the number of moles of lipid per unit surface area of the micelle and that the micelle surface area is given by the surface areas of the constituent headgroups present. This form is readily accessible for application to experimental data because it can be deployed without further assumption and only bulk concentrations and molecular surface areas need be known. It can be used to determine the individual kinetic parameters. (ii) The plots of the product formed vs. time were found to be linear. The duration over which linearity is present increases with the concentration of bile salt. At high bile salt to lipid ratio (>5), linearity extends to about 10 min. Presence of linearity shows that the substrate replenishment occurs at a rate faster than the catalytic rate and that the kinetic parameters may be treated as constant in the linear region. Therefore, microstructural variation due to products formed notwithstanding, one may extract kinetic parameters from the initial linear regions of the reaction progress curves. Microstructural variation due to polydispersity is not an issue because the products measured are from encounters with the entire population of micelles. (iii) The activity was found to depend on the surface substrate concentration as quantified by Eq. (17), in accordance with the kinetic scheme that treats the interface as a cofactor [3]. The parameters defining the kinetics, K_S, K_M, and k_3 were individually determined and found to depend on detergent to lipid ratio. The micelle microstructure also depends on the concentration of detergent. Therefore the role of the microstructure is implicitly present through the kinetic parameters. (iv) Time-resolved fluorescence quenching techniques were employed to characterize the mixed micelles and the information was used to interpret the kinetic data. TRFQ results showed that the micelle size decreases with increase in the bile salt to lipid ratio. The micelles were broadly classified as large micelles at lower bile salt to lipid ratio (<5) and small micelles at higher ratios. The enzyme–micelle dissociation rate is higher for the smaller micelles. This observation is consistent with the argument that as micelles become smaller the available binding area decreases leading to a weak binding and the enzyme dissociation rate increases. This work thus identifies the role of the micelle microstructure in the existence of the conditions for steady state. Decrease in the available overlap area as micelles get smaller is one rational explanation for the change in the value of K_S between the large and small micelles. The decrease in the catalytic rate k_3, between large and small micelles needs further investigation. A possible explanation may involve the conformation imposed on the lipid in the micelle, which may change according to micelle size. The generality of the kinetic

model, here presented, with the substrate concentration quantified as in Eq. (17) remains to be established. It opens a line of investigation for kinetics of enzymatic lipolysis including studies with related phospholipases and other lipid substrates.

Acknowledgement

Support for this project by a grant from NIH under the contract S06 GM48680 is gratefully acknowledged. R.R. and J. H. thank the CSUN Office of Research and Sponsored projects and the College of Science and Mathematics for their support of the project.

Appendix A. Time-resolved quenching decay data fitting and analysis

The fitting of Eq. (18) to the quenched fluorescence decay data is complicated if micelles are polydisperse. Lipid/bile salt mixed micelles are generally found to be polydisperse. Polydispersity in micelle size would give rise to a distribution in k_q values and possibly in k_0 as well [33]. Two methods are available that derive average properties of polydisperse micelles from TRFQ data [33,34]. In this work we adopt a combination of a lifetime distribution analysis and the method of Almgren and Lofroth [33,34]. The Infelta model is used as a first approximation to fit the decay data. A general problem encountered in fits with multiple parameters, is that several sets of parameters can give good fits. We select the set of k_0, k_q, and A_3 for which the goodness of fit indicator, χ^2, is a minimum and the random residuals plot shows no visible systematic feature. First, the decay data are subjected to a lifetime distribution analysis in which the decay curve is fit to a sum of one hundred exponential decays. Our results show a clear presence of two distinct distributions around a longer lifetime of about 320 to 380 ns typical of the lifetime of unquenched pyrene fluorescence in degassed micellar solutions and a shorter lifetime less than about 100 ns which is attributed to the quenching of pyrene fluorescence in micelles containing quenchers. The longer lifetime is used as fixed value of k_0^{-1} and the shorter lifetime T_2 as the initial (zero order) fixed value of k_q^{-1} in the Infelta model, Eq. (18), and a fit to the decay curve is performed to recover the zero order value of A_3, denoted by A_3^0. The quenching constant, k_q, is the quenching rate due to one quencher and is strictly not equal to T_2^{-1}, because T_2^{-1} represents the decay rate in a collection of micelles some of which may have two or more quenchers. Occurrence of micelles with more than one quencher, as given by the Poisson distribution, means that the rate T_2^{-1} is not just due to one quencher. At low quencher concentrations, however, single micelle occupancy is far more probable than multiple occupancy and $k_q = T_2^{-1}$ becomes a good zero order approximation. The zero order k_q is denoted by k_q^0. In the second iteration, A_3 is fixed at A_3^0 and the next k_q is determined. Several iterations are performed alternately fixing A_3 and k_q until the values converge and a $\chi^2 \approx 1$ and a residuals plot with no visible periodicity are obtained. Fig. 7 is an example of the results of such a fitting procedure.

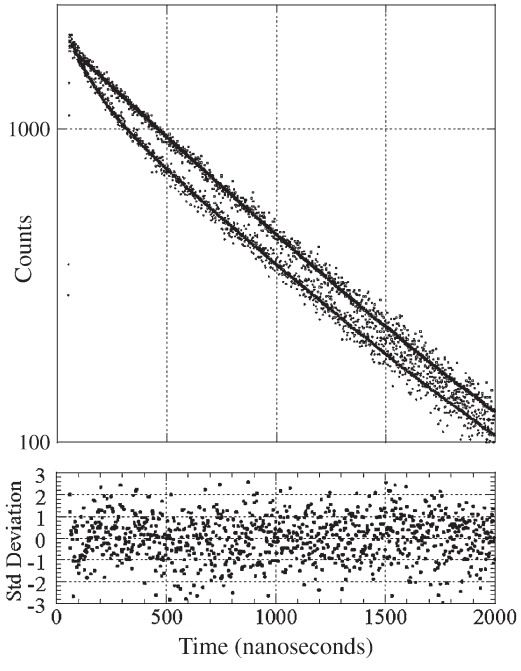

Fig. 7. Time-resolved fluorescence decay data in a sample with [DMPC]=4 mM and [NaDC]=12.5 mM. The curves in the upper graph are the fluorescence photon counts data and fit of pyrene fluorescence in the absence of quenchers (upper curve) and quenched decay data and fit in the presence of quenchers (lower curve). The lower panel shows the residuals of the fit of the Infelta model (Eq. (18)) to the quenched decay data. The quencher is the nitroxide radical attached to a lipid (Fig. 1).

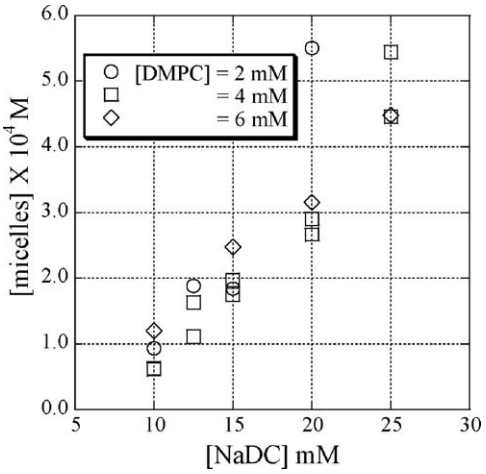

Fig. 8. [Micelles] vs. [NaDC] to calculate the IMC of NaDC using Eq. (14).

The concentration of micelles, [micelles], derived from the fitted A_3, and using Eq. (19) depends on quencher concentration as a consequence of polydispersity [33,34]. The average [micelles] is then computed from the solution to a truncated series equation, which expresses the quencher averaged aggregation number as a power series of the quencher concentration with the central moments of the micelle size distribution as the coefficients [33,34]. For any given sample composition and concentration, TRFQ measurements were conducted for two quencher concentrations. The average

[micelles] was then computed from two quencher dependent values as,

$$[\text{micelles}] = \frac{[Q_2]-[Q_1]}{\frac{[Q_2]}{[Q_1]}A_3^1 - \frac{[Q_1]}{[Q_2]}A_3^2}, \quad \text{(A1)}$$

where A_3^1 and A_3^2 are the results for A_3 of fitting of Eq. (18) to the TRFQ decay curves at two quencher concentrations $[Q_1]$ and $[Q_2]$, respectively. The value of $[Q_2]$ was about twice $[Q_1]$ and $[Q_1]$ was such that the number of quenchers per micelle, A_3^1, was between 0.3 and 0.4. Only the TRFQ data of the [DMPC]= 6 mM series was treated with Eq. (A1). The lower [DMPC] series showed less than a 20% variation between the two quencher concentrations.

The quenching constant k_q (Fig. 4)) showed a variation of <10% between the two quencher concentrations. Applying Eq. (14) to the dependence of the concentration of [micelles] on the total bile salt concentration, the bile salt aggregation numbers and the IMC were determined. The plots are presented in Fig. 8 and the derived data in Table 1.

Appendix B. Uncertainties and errors

The parameter values that yield a good fit span a range which is then adopted as the uncertainty in those numbers. The measured values of k_q and [micelles] in this work are thus each quoted with uncertainties of 20%. To determine the uncertainty in the activity, six different samples of the same concentration were prepared and the specific activity was measured for these samples over a period of three days. The standard deviation in the measured activity is less than 5%. The error bars on the activity in Figs. 3 and 5 are due to the errors in the determination of the slopes of the reaction progress curves shown in Fig. 2. These are less than about 1% for [NaDC]>15 mM. Larger errors are found for the lower [NaDC] and are shown in the figures.

References

[1] O.G. Berg, M.H. Gelb, M.-D. Tsai, M.K. Jain, Interfacial enzymology: the secreted phospholipase A2-paradigm, Chem. Rev. 101 (9) (2001) 2613–2653.
[2] W.A. Pieterson, J.C. Vidal, J.J. Volwerk, G.H. de Haas, Zymogen-catalyzed hydrolysis of monomeric substrates and the presence of a recognition site for lipid–water interfaces in phospholipase A2, Biochemistry 13 (1974) 1455–1460.
[3] R.A. Deems, B.R. Eaton, E.A. Dennis, Kinetic analysis of phospholipase A2 activity toward mixed micelles and its implications for the study of lipolytic enzymes, J. Biol. Chem. 250 (23) (1975) 9013–9020.
[4] W.J. Hoffman, M. Vahey, J. Hajdu, Pancreatic porcine phospholipase A2 catalyzed hydrolysis of phosphatidycholine in lecithin–bile salt mixed micelles: kinetic studies in a lecithin–sodium cholate system, Arch. Biochem. Biophys. 221 (2) (1983) 361–370.
[5] M.K. Jain, O. Berg, The kinetics of interfacial catalysis by phospholipase A2 and regulation of interfacial activation: hopping versus scooting, Biochim. Biophys. Acta 1002 (1989) 127–156.
[6] M.K. Jain, J. Rogers, H.S. Hendrickson, O.G. Berg, The chemical step is not rate-limiting during hydrolysis by PLA2 of mixed micelles of phospholipid and detergent, Biochemistry 32 (1993) 8360–8367.
[7] D.E. Cohen, G.M. Thurston, R.A. Chamberlin, G.B. Benedek, M.C. Carey, Laser light scattering evidence for a common wormlike growth structure of mixed micelles in bile salt- and straight-chain detergent–phosphatidylcholine aqueous systems: relevance to the micellar structure of bile, Biochemistry 37 (42) (1998) 14798–14814.
[8] R. Rosseto, J. Hajdu, A rapid and efficient method for migration-free acylation of lysophospholipids: synthesis of phosphatidylcholines with *sn*-2-chain-terminal reporter groups, Tetrahedron Lett. 46 (161) (2005) 2941–2944.
[9] O.H. Lowry, N.J. Rosebrough, A. Lewis Farr, R.J. Randall, Protein measurement with the folin phenol reagent, J. Biol. Chem. 193 (1951) 265–275.
[10] W. Nieuwenhuizen, H. Kunze, G.H. De Haas, Phospholipase A2 (phosphatide acylhydrolase, EC 3.1.1.4) from porcine pancreas, Methods Enzymol. 32B (1974) 147–154.
[11] M.H. Gehlen, F.C. De Schryver, Time-resolved fluorescence quenching in micellar assemblies, Chem. Rev. 93 (1) (1993) 199–221.
[12] M. Almgren, J.E. Löfroth, Determination of micelle aggregation numbers and micelle fluidities by time-resolved fluorescence quenching studies, J. Colloid Interface Sci. 81 (1981) 486–499.
[13] M. Almgren, in: M. Grätzel, K. Kalyanasundaram (Eds.), Kinetics and Catalysis in Microheterogeneous Systems, Marcel Dekker, Inc., New York, 1991, pp. 63–113.
[14] B.L. Bales, R. Zana, Characterization of micelles of quaternary ammonium surfactants as reaction media: dodeclytrimethylammonium bromide and chloride, J. Phys. Chem., B 106 (8) (2002) 1926–1939.
[15] P.P. Infelta, M. Grätzel, J.K. Thomas, Luminescence decay of hydrophobic molecules solubilized in aqueous micellar systems. Kinetic model, J. Phys. Chem. 78 (2) (1974) 190–195.
[16] R. Ranganathan, M. Peric, B.L. Bales, Time-resolved fluorescence quenching measurements of the aggregation numbers of normal sodium alkyl sulfate micelles well above the critical micelle concentrations, J. Phys. Chem. 102 (1998) 8436–8439.
[17] R. Ranganathan, L. Tran, B.L. Bales, Surfactant and salt induced growth of normal alkyl sodium sulfate micelles well above their CMC, J. Phys. Chem., B 104 (2000) 2260–2264.
[18] R. Ranganathan, M. Peric, R. Medina, U. Garcia, B.L. Bales, M. Almgren, Size, hydration, and shape of SDS/heptane micelles investigated by TRFQ and ESR, Langmuir 17 (2001) 6765–6770.
[19] R. Ranganathan, C. Giongo, M.S. Bakshi, B.L. Bales, J. Hajdu, Phospholipid containig mixed micelles: characterization of diheptanoyl-phosphatidylcholine (DHPC) and sodium dodecyl sulfate and DHPC and dodecyl trimethylammonium bromide, Chem. Phys. Lipids 135 (2005) 93–104.
[20] E. Szajdzinska-Pietek, J.L. Gebicki, Location of hydrophobic solutes in SDS micelles and the effect of tetraalkylammonium counterions on the structure of the head-group region. Pulse radiolytic study on scavenging of hydrated electrons, J. Phys. Chem. 99 (36) (1995) 13500–13504.
[21] E. Szajdzinska-Pietek, M. Wolszczak, Quenching of pyrene fluorescence by amphiphilic nitroxide radicals embedded in cationic micelles, Chem. Phys. Lett. 270 (1997) 527–532.
[22] A.E. Tringali, S.K. Kim, H.C. Brenner, ODMR and fluorescence studies of pyrene solubilized in anionic and cationic micelles, J. Lumin. 81 (1999) 85–100.
[23] S. Matzinger, D.M. Hussey, M.D. Fayer, Fluorescent probe solubilization in the headgroup and core regions of micelles: fluorescence lifetime and orientational relaxation measurements, J. Phys. Chem., B 102 (1998) 7216–7224.
[24] D. Banerjee, P.K. Das, S. Mondal, S. Ghosh, S. Bagchi, Interaction of ketocyanine dyes with cationic, anionic and neutral micelles, Photochem. Photobiol. 98 (1996) 183–186.
[25] S. Reekmans, H. Luo, M. Van der Auweraer, F.C. De Schryver, Influence of alcohols and alkanes on the aggregation behavior of ionic surfactants in water, Langmuir 6 (1990) 628–737.
[26] S.A. Tatulian, Toward understanding interfacial activation of secretory phospholipase A2: membrane surface properties and membrane-induced structural changes in the enzyme contribute synergestically to PLA_2 activation, Biophys. J. 80 (2001) 789–800.

[27] G. Basanez, J.-L. Nieva, F.M. Goni, A. Alonso, Origin of the lag period in the phospholipase C cleavage of phospholipids in membranes. Concomitant vesicle aggregation and enzyme activation, Biochemistry 35 (1996) 15183–15187.
[28] F.M. Goni, A. Alonso, Structure and functional properties of diacylglycerols in membranes, Prog. Lipid Res. 38 (1999) 1–48.
[29] C.H. Spink, K. Muller, J.M. Stutevant, Precision scanning calorimetry of bile salt–phosphatidylcholine micelles, Biochemistry 21 (1982) 6598–6605.
[30] J. Santhanalakshmi, G. Shantha Lakshmi, V.K. Aswal, P.S. Goyal, Small-angle neutron scattering study of sodium cholate and sodium deoxycholate interacting micelles in aqueous solutions, Proc. Indian Acad. Sci., Chem. Sci. 113 (2001) 55–62.
[31] J.W. Nichols, Phospholipid transfer between phosphatidylcholine–taurocholate mixed micelles, Biochemistry 27 (1988) 3925–3931.
[32] D.A. Fullington, D.G. Shoemaker, J.W. Nichols, Characterization of phospholipid transfer between mixed phospholipid–bile salt micelles, Biochemistry 29 (1990) 879–886.
[33] M. Almgren, J.E. Löfroth, Effects of polydispersity on fluorescence quenching in micelles, J. Chem. Phys. 76 (5) (1982) 2734–2743.
[34] A. Siemiarczuk, W.R. Ware, Y.S. Liu, A novel method for determining size distributions in polydisperse micelle systems based on the recovery of fluorescence lifetime distributions, J. Phys. Chem. 97 (1993) 8082–8091.